



HAL
open science

Optimization of a micronekton model with acoustic data

Patrick Lehodey, Anna Conchon, Inna Senina, Réka Domokos, Beatriz Calmettes, Julien Jouanno, Olga Hernandez, Rudy Kloster

► To cite this version:

Patrick Lehodey, Anna Conchon, Inna Senina, Réka Domokos, Beatriz Calmettes, et al.. Optimization of a micronekton model with acoustic data. *ICES Journal of Marine Science*, 2015, 72 (5), pp.1399 - 1412. 10.1093/icesjms/fsu233 . hal-01496775

HAL Id: hal-01496775

<https://hal.science/hal-01496775>

Submitted on 1 Mar 2024

HAL is a multi-disciplinary open access archive for the deposit and dissemination of scientific research documents, whether they are published or not. The documents may come from teaching and research institutions in France or abroad, or from public or private research centers.

L'archive ouverte pluridisciplinaire **HAL**, est destinée au dépôt et à la diffusion de documents scientifiques de niveau recherche, publiés ou non, émanant des établissements d'enseignement et de recherche français ou étrangers, des laboratoires publics ou privés.

Optimization of a micronekton model with acoustic data

Patrick Lehodey^{1*}, Anna Conchon¹, Inna Senina¹, Réka Domokos², Beatriz Calmettes¹,
Julien Jouanno³, Olga Hernandez⁴ and Rudy Kloser⁵

¹ Space Oceanography Division, CLS, 8-10 rue Hermes, Ramonville 31520, France

² Ecosystems and Oceanography Division, Pacific Islands Fisheries Science Center, NMFS, NOAA, 2570 Dole Street, Honolulu, HI 96822, USA

³ LEGOS, 18, av. Edouard Belin, Toulouse 31400, France

⁴ LOCEAN, 4 Place Jussieu, Paris 75252, France

⁵ CSIRO Marine and Atmospheric Research, GPO Box 1538, Hobart 7005, Australia

*: Corresponding author : Patrick Lehodey, Tel: +33 561 393 770 ; Fax: +33 561 393 782 ;
email address : plehodey@cls.fr

Abstract:

In the pelagic foodweb, micronekton at the mid-trophic level (MTL) are one of the lesser known components of the ocean ecosystem despite being a major driver of the spatial dynamics of their predators, of which many are exploited species (e.g. tunas). The Spatial Ecosystem and Population Dynamics Model is one modelling approach that includes a representation of the spatial dynamics of several epi- and mesopelagic MTL functional groups. The dynamics of these groups are driven by physical (temperature and currents) and biogeochemical (primary production, euphotic depth) variables. A key issue to address is the parameterization of the energy transfer from the primary production to these functional groups. We present a method using *in situ* acoustic data to estimate the parameters with a maximum likelihood estimation approach. A series of twin experiments conducted to test the behaviour of the model suggested that in the ideal case, that is, with an environmental forcing perfectly simulated and biomass estimates directly correlated with the acoustic signal, a minimum of 200 observations over several time steps at the resolution of the model is needed to estimate the parameter values with a minimum error. A transect of acoustic backscatter at 38 kHz collected during scientific cruises north of Hawaii allowed a first illustration of the approach with actual data. A discussion followed regarding the various sources of uncertainties associated with the use of acoustic data in micronekton biomass.

Keywords: acoustic ; maximum likelihood estimation ; micronekton ; model optimization ; modelling ; Pacific ocean ; SEAPODYM

Introduction

The development of marine ecosystem models is providing new useful tools and products in investigating the combined effects of fishing, environmental variability and the impacts of climate changes on species of interest; in particular, exploited or protected species (e.g., De Young et al. 2004; Fulton 2010; Lehodey et al. 2008; Plagányi 2007; Senina et al. 2008; Dueri et al. 2012; Sibert et al. 2012). The first necessary step in the development of such ocean ecosystem models is to produce reliable predictions of the physical-biogeochemical oceanic environment. Physical ocean-circulation models are now providing realistic simulations of the ocean by assimilating large amounts of sea surface satellite and depth profile data (e.g., ARGO program) to produce reanalyses of the past and present ocean state at high resolution. The modeling of lower trophic levels, that is, the phyto- and zooplankton, is also rapidly progressing (Brasseur et al. 2010, Holt et al. 2014) and should soon provide operationally realistic outputs to connect these ocean models to the higher biological levels. As an immediate alternative, primary production by phytoplanktonic groups can be inferred from satellite data (e.g., Behrenfeld and Falkowsky 1997), with the advantage of providing a realistic description of mesoscale activity.

While the modeling of these physical and biological variables is well advanced, this is not the case however, for the epi- and mesopelagic mid-trophic level (MTL) organisms (macrozooplankton and micronekton) that are a critical component in the oceanic ecosystem. By definition, micronekton are small organisms (~1-20 cm or g) that can swim; however, their small sizes are still strongly impacted by oceanic circulation from large to mesoscale. They distribute between the surface and the deep layers with some groups of species migrating every night and day between these vertical layers. Predators have adapted their behavior to chase these forage species by using their physical and physiological skills for accessing the different layers. These predators include many exploited stocks (e.g., tunas and swordfish) and protected species (e.g. turtles, seabirds, sharks and marine mammals), and realistic simulations of micronektonic prey would provide a key explanatory variable that is currently missing to better understand individual behavior and population dynamics. Additionally, micronektonic organisms are a major source of grazing of zooplankton and are predators of eggs and larvae drifting in the pelagic environment, including those of the exploited species. Micronekton also interact with the carbon cycle, including the CO₂ released in the atmosphere by human activity, as they contribute to the production of particular organic matter (POC) that is recycled either in the microbial loop or stored by sinking to the deep ocean (Holt et al., 2014). Thus, micronekton are central to the understanding and modelling of oceanic ecosystems and there is a pressing need for increased knowledge and for models pertaining to their biomass estimate and ecological role.

Several modeling approaches can be used to estimate micronekton biomass (e.g., Kitchell et al. 1999, Jennings et al. 2008; Maury 2010; Lehodey et al., 2010a). The Spatial Ecosystem And Population Dynamics Model (SEAPODYM) in this study includes a representation of several MTL functional groups, i.e., the epi- and meso-pelagic micronekton, to describe the prey fields of tuna and other large pelagic predators (Lehodey et al., 2010a). This micronekton model has been used in several applications on tuna species (Lehodey et al. 2008; Senina et al. 2008; Lehodey et al., 2010b, 2013; Briand et al 2011; Sibert et al. 2012), and its outputs used to investigate habitats and movements of other large oceanic species (Abecassis et al 2013; Lambert et al., 2014).

A key issue in the SEAPODYM modelling approach is to parameterize the energy transfer from the primary production to the functional groups of micronekton. A preliminary parameterization (Lehodey et al., 2010a) was achieved based on a first compilation of existing data in the literature and a Pacific basin-scale simulation at coarse resolution (1 deg × month). A more rigorous approach requires the use of data assimilation methods to optimize the parameters using acoustic data that provides a synoptic view of micronekton biomass in the vertical layers of the ocean. Over the recent years, acoustic

estimates of micronekton biomass has received increased attention, and many acoustic transects are collected at basin scales by various research and fishing vessels. An effort of standardization between these different data sources (e.g., IMOS project: <http://imos.org.au/anmnacous.html>) should fill the important gap in the understanding of basin scale mid-trophic biomass and distribution providing data to initialize and assimilate into ecological models.

Here, we present a methodology for a parameter optimization approach based on assimilation of acoustic data in the MTL model. Assimilation experiments with the MTL model at high-resolution in the Pacific Ocean are used to validate the method and to highlight the need for collecting and standardizing such data. After a series of twin experiments conducted to test the behavior of the model, a transect of acoustic backscatter at 38 kHz collected during scientific cruises north of Hawaii illustrates the approach. We assumed that the intensity of the acoustic signal is proportional to the density of micronekton. This is not always true, e.g. due to resonant scattering diel shifts, and has been identified by the acoustic community as needing more research (e.g. Handegard et al 2013).

Material and Methods

1. The mid-trophic model

In its present version, the SEAPODYM MTLs sub-model includes 3 vertical layers and 6 functional groups characterized by their vertical behavior, i.e., with or without occurrence of diel migration between three vertical layers. Recruitment, ageing, mortality and passive transport with horizontal currents are modeled by a system of Advection-Diffusion-Reaction equations, taking into account the vertical behavior of organisms (Lehodey et al., 2010a). Since the dynamics are represented by a relationship of temperature-linked time development, only six parameters in the model have to be estimated. The first one (E) defines the total energy transfer between primary production and all the MTL groups. The other parameters are the relative coefficients (E'_n) redistributing this energy through the different components (the sum of which being 1). The parameterization of E requires absolute biomass estimates of MTL, while the matrix of E'_n coefficients can be estimated simply using relative day and night values integrated in the three vertical layers of the model. The 6 parameters of the MTL model have been initially tuned according to very limited *in situ* data and information from the literature (Lehodey et al., 2010a).

2. Terminology and definition of vertical layers

In its first version, the layers of the model were conveniently named as epi-, meso- and bathypelagic (Lehodey et al 2010a). However, the names of the functional groups were revised (Fig. 1) to comply with the standard terminology that defines the bathypelagic layer below 1000 m. The 3 vertical layers are therefore renamed as epipelagic, upper- and lower- mesopelagic layers. They have been defined relatively to the euphotic depth (Z_{eu}), assuming the vertical migration of micronektonic organisms is primarily driven by light. When comparing acoustic profiles with Z_{eu} (Fig. 1) in the region of study, the epipelagic layer appeared to extend deeper than the euphotic depth computed according to the VGPM model of Behrenfeld and Falkowski (1997). Thus the first layer was computed using $1.5 \times Z_{eu}$. The second and third layer boundaries were defined as 3 times and 7 times the depth of the first layer (with a maximum set at 1000 m) based on visual inspection of acoustic transects (Fig. 1). The definition of vertical layers, based on the euphotic depth and the few available acoustic transects for this study, could evolve while more data becomes available (see discussion). Each MTL functional group is identified by the layer that is inhabited by its organisms during the day and night. With this terminology the epipelagic group is called MTL1.1 since it is always in the first layer, while the highly

migrant lower mesopelagic group becomes MTL3.1, i.e., inhabiting the third layer during the day and moving up to the surface layer at night (Fig. 1).

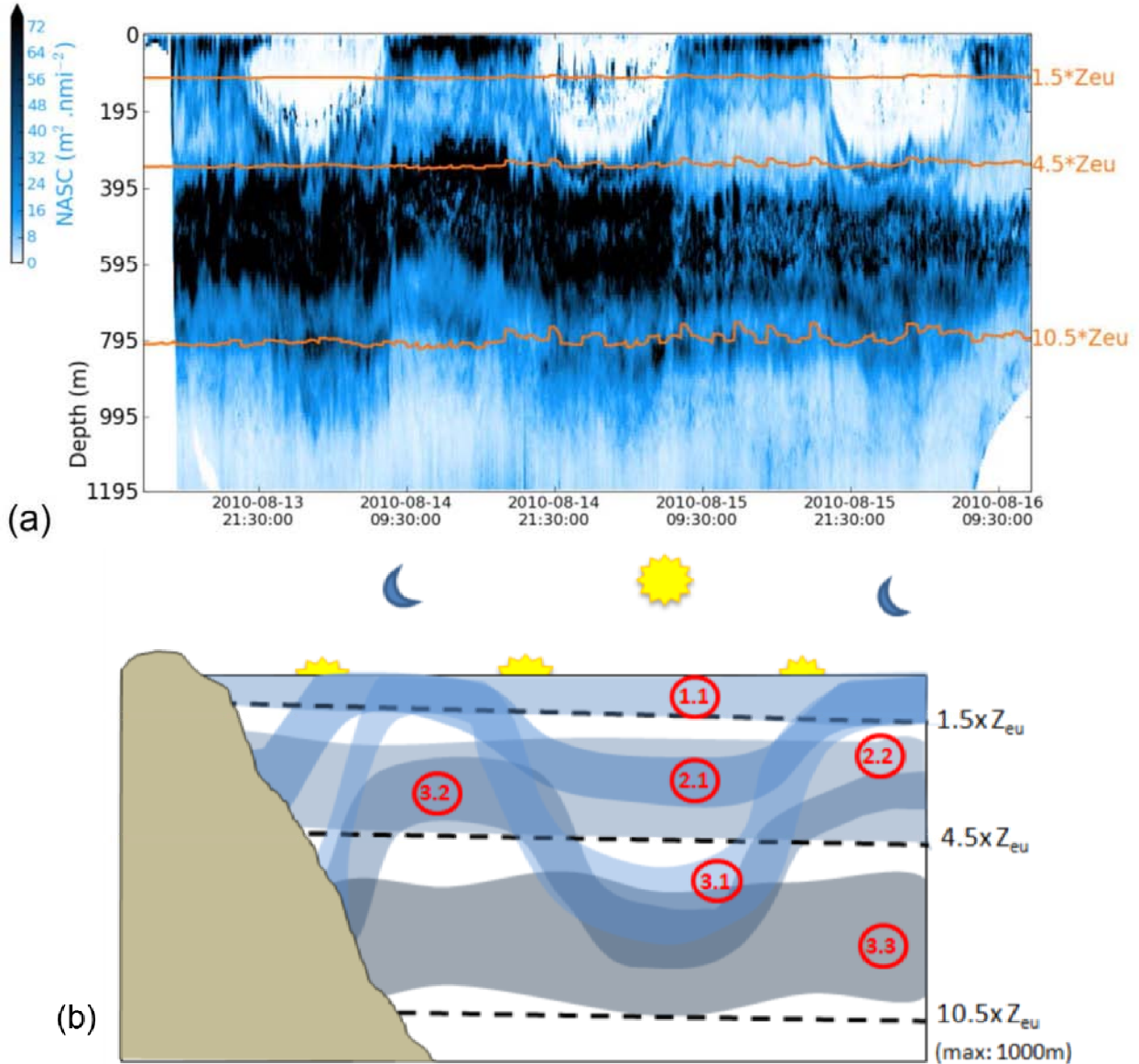


Figure 1: Identification of MTL functional groups on acoustic echogram (a) and conceptual model (b), revised from Lehodey et al. (2010a). 1.1: Epipelagic; 2.1: Migrant upper mesopelagic; 2.2: Upper mesopelagic; 3.1: Highly-migrant lower mesopelagic; 3.2: Migrant lower mesopelagic; 3.3: Lower mesopelagic.

3. Model domain and forcing

Acoustic transect data are strongly influenced by the mesoscale activity and represent very detailed but also a very small portion of the ocean. A realistic high-resolution ocean physics and biogeochemistry feedback is needed to extract the largest information from data used in the optimization approach. We

used the ocean reanalysis GLORYS (glorysproducts@mercator-ocean.fr). With the project GLORYS (GLobal Ocean ReanalYsis and Simulations), supported by the French Groupe Mission Mercator Coriolis, a first eddy resolving global ocean reanalysis has been produced for the 2002-2009 period with the ocean general circulation model configuration ORCA025 NEMO, i.e., a spatial resolution of $\frac{1}{4}^\circ$ (Barnier et al., 2006). The assimilation method is based on a reduced order Kalman filter (SEEK formulation, Pham et al. 1998) adapted to eddy resolving global ocean model configuration (Tranchant et al., 2008). The GLORYS.2v1 reanalysis was updated for the recent period with the operational Mercator-Ocean (<http://www.mercator-ocean.fr/eng>) global ocean model PSY3 that is using the same grid and assimilation scheme than GLORYS. Because the ocean circulation model assimilates satellites (SST and altimetry) and *in situ* data, predicted fields of temperature and currents are globally coherent with those of primary production derived from ocean color data (Fig. 2), using the VGPM model of Behrenfeld and Falkowsky (1997).

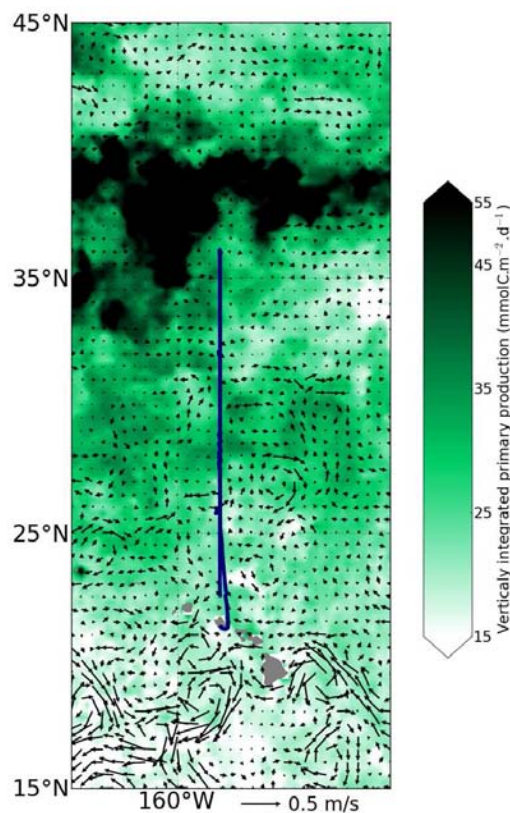


Figure 2: Snapshots showing the derived primary production computed following the VGPM model of Behrenfeld and Falkowsky (1997) with superimposed surface currents (average in the euphotic layer) predicted in GLORYS2v1 reanalysis (glorysproducts@mercator-ocean.fr) and the Hawaiian Transect.

The model computes spatial distribution of production and biomass of each functional group at the resolution of the physical model. The total biomass for each layer during day-time and night-time was computed by adding the different components accordingly. For instance, the surface layer is inhabited only by the epipelagic group during the day but the sum of epipelagic, upper-migrant mesopelagic and highly-migrant lower mesopelagic groups during the night. These predictions can be compared to acoustic biomass estimates by layer during nights and days. Though the original domain of the model is

global between latitude 66.5°N and 66.5°S, a subdomain has been extracted for optimization in the North Pacific to save computational time, with geographical coordinates 66.5°N-0°N, 90°E-70°W and closed boundary conditions.

4. Acoustic data

A shipboard survey was conducted in March 2009 along the longitude 158°W from 22°N to 36°N (so-called “Hawaiian transect” in the following text) that has been used for optimization experiments (Fig. 2). Bioacoustic signals were collected continuously down to 1200 m with a hull-mounted split-beam Kongsberg Maritime AS Simrad EK60 system (Horten, Norway), operating at the 38, 70, and 120 kHz frequencies. The EK60 system was calibrated prior to data collection with a 38.1 mm tungsten carbide sphere according to standard methods (Foote et al., 1987). As the higher frequency signals attenuate shallower than the bottom of the lower mesopelagic layer, only 38-kHz full-resolution acoustic data were used. Volume backscattering coefficients (S_v , in dB re 1 m⁻¹) were converted into nautical area scattering coefficient (NASC, in m² nmi⁻²) values and assumed proportional to micronekton biomass (Mac Lennan et al., 2002). Since the 38 kHz frequency signal is dominated by micronektonic organisms (Handegard et al. 2013), the integration of NASC is believed to be representative of the total biomass of the 6 functional groups of the model. However, a series of potential biases occur that are presented in the discussion. Also, the position of the transducer below the hull prevents any recording from the first 5 m, while data about 10 m from the transducer face is unreliable due to nonlinearities in the nearfield. In addition to the loss of recording in the upper 15 m, water displaced in front of the vessel together with the possible escapement behavior of organisms likely leads to a negative bias in biomass estimates in the surface layer. To compensate this bias, we decided to correct the signal by adding 5% of total biomass in the epipelagic functional group, considering that about 5-10% of the total biomass should be in the first 100 m during daytime in the tropical and subtropical ocean (e.g., Grandperrin 1975; Irigoien et al. 2014).

After a few tests, the Hawaiian transect showed a low signal-to-noise ratio (Fig. 3) thereby making convergence in the model difficult. This noise is a result of the cavitations and bubble dropout, characterized by high frequency localized extreme values and was filtered using a running geometric mean (eq. 1) with a window range $(1+2f)$ of 7 bins for each vertical layer at resolution of 10 m.

$$NASC'(d, t) = \left(\prod_{t'=t-f}^{t'+f} NASC(d, t') \right)^{1/(1+2f)} \quad \text{eq. 1}$$

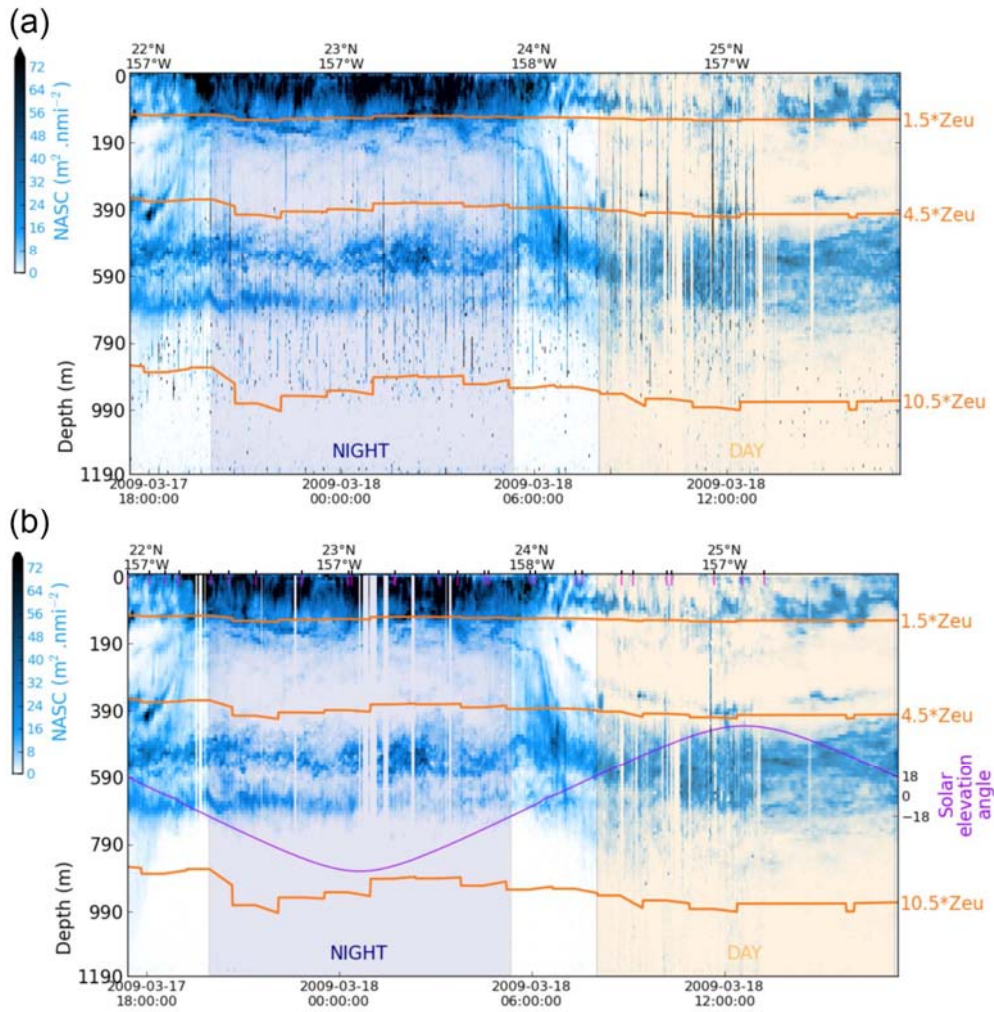


Figure 3: Example of a portion of acoustic transect before (a) and after (b) processing the data (both averaged over a minute). After the vertical layers have been defined the signal strength is vertically integrated and then averaged at the spatial resolution of the grid of the model ($1/4^\circ$) after excluding the sunset and sunrise time periods. The orange lines delineate the vertical layers boundaries based on the euphotic depth. The purple line shows the variation of the solar elevation angle (which is used to discriminate between night and day) through the day. Small ticks (black and pink) on the horizontal axis indicate the position each five horizontal cells of the model grid.

5. Optimization approach

The simple modelling approach used to describe the MTL components with a limited number of parameters helps implementing a method of parameter estimation by using data assimilation. The matrix of E'_n coefficients can be estimated simply using relative day and night values of acoustic backscatter integrated in each of the 3 vertical layers of the model. The energy transfer coefficients are optimized to fit the relative ratios of micronekton biomass (or NASC) between layers changing during day and night periods. First, the NASC values are integrated at the resolution of the model in space (in each cell grids of the model and in each layer) and time (during night-time and day-time, excluding transition periods). Based on the sum of values for the 3 layers, the signal of the first layer is increased

by 5%. Then, the ratio (ρ) for each layer (K) and night or day period (Ω) is computed relatively to the corrected sum of the 3 layers (eq. 2) defined by their upper (Z_u) and deeper (Z_d) vertical boundaries:

$$(\rho_K)_{i,j,t,\Omega}^{obs} = \frac{\int_t \int_i \int_j \int_{Z_d^{(K)}}^{Z_u^{(K)}} (NASC(x,y,z,t)I_\Omega) dz dy dx dt}{\int_t \int_i \int_j \int_0^{Z_u^{(3)}} (NASC(x,y,z,t)I_\Omega) dz dy dx dt} \quad (\text{eq. 2})$$

where, (i, j) is the position (the cell) in the grid of the model domain, t the time (in the model resolution), Ω the part of the day (night or day), and I_Ω the identity function (1 in Ω , 0 elsewhere). Day and night periods are defined based on the solar elevation angle (Downey 1990; see <https://pypi.python.org/pypi/pyephem/> for Python language scripts) with day when the altitude is $> 18^\circ$ and night with altitude $\leq 18^\circ$ (Fig. 3).

The integration of acoustical signal along a transect is illustrated in Fig. 3. According to the local time of the day, these values can be compared to the relative distribution of predicted biomass in the same layers, accounting for the different combination of MTL components due to vertical migration. Sunset and sunrise time periods are excluded by the definition using solar altitude.

Observed ratios (ρ^{obs}) for each layer K are compared to the model predictions (ρ^{pred}). The predicted ratios in grid cell (i, j) at time t , for the part of the day Ω , in a layer K is the sum of the biomass of each group inhabiting the layer K , at this position and time and divided by the total biomass in all layers (eq. 3):

$$(\rho_K)_{i,j,t,\Omega}^{pred} = \frac{\sum_{\substack{1 \leq n \leq 6 \\ k(n,\Omega)=K}} B_{i,j,t}^n}{\sum_{1 \leq n \leq 6} B_{i,j,t}^n} \quad (\text{eq. 3})$$

with n the functional group, B^n the biomass of the group n , and $k(n, \Omega)$ the layer inhabited by group n during the period of day Ω .

The optimization approach will search for the optimal set of parameters E'_n that provides the best fit between observation and prediction. Since the approach use relative ratio of integrated acoustic signal, it is possible to include data from various sources and without standardization. However, for the parameterization of E , i.e., the total energy transfer that controls the level of absolute biomass, it would be necessary to use calibrated biomass estimates. They need to combine acoustic and micronekton net sampling allowing to convert backscatter values in micronekton biomass after careful discrimination between various recorded patches of records. This objective is not included in the present approach. Nevertheless, based on a detailed acoustic study (Kloser et al 2009), the previous estimate of biomass appeared largely underestimated and the value of E was increased (i.e., manually tuned to a value of 0.04) to fit these recent estimates.

The optimization approach uses the adjoint technique with the quasi-Newton gradient method to minimize the cost function (L) as described in Senina et al. (2008), but the new likelihood function required several modifications of the adjoint code.

First, the distribution of observed ratios suggest a log-normal distribution for data in the first 2 layers either during day or night, but not for the deepest (lower mesopelagic) layer. However, since the sum of ratios of the three layers is necessary at each given location and time, it was possible to use the complementary distribution to 1 (i.e., $1 - \rho_3^{obs}$) which in that case become much closer of the log-normal distribution. Quantile-Quantile plots (Q-Q plot, Fig. 4) presenting the fit between observations and theoretical distributions confirmed that these distributions of observed ratios (ρ^{obs}) are close to the log-normal distribution ($R^2 > 0.9$).

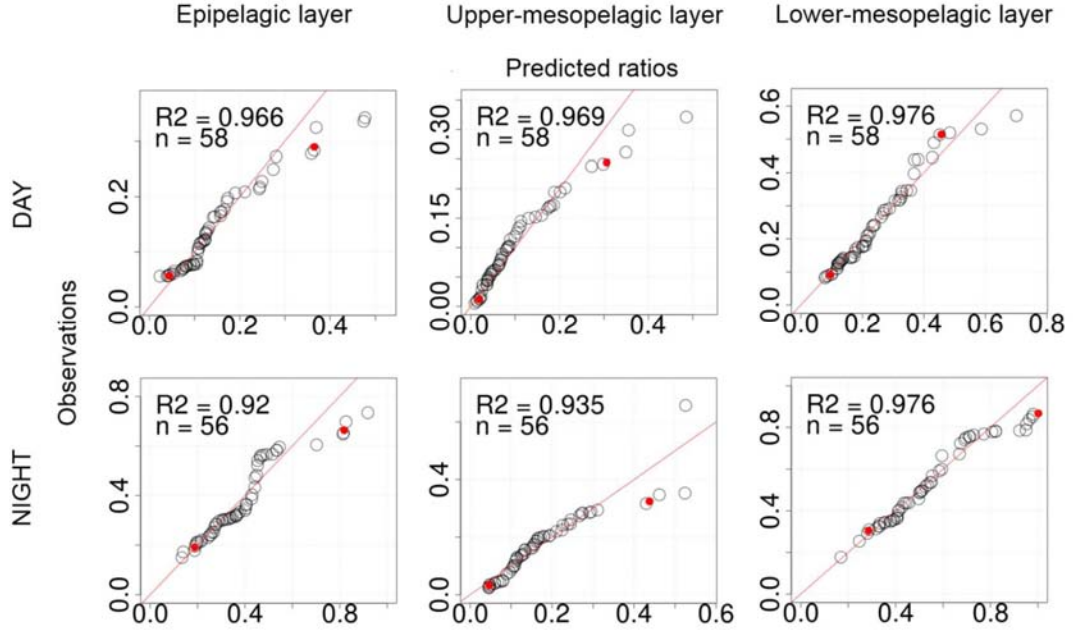


Figure 4: Quantile-quantile plot of the observed ratios by layer and period of day using log-normal distribution for predicted ratios of epi- and upper mesopelagic layers and the complementary distribution ($1 - \rho_3^{obs}$) for lower mesopelagic layer. Black dots indicate the 5th and 95th percentile of the distribution.

Based on this distribution the cost function is built as the sum of the negative log-likelihood computed for each layer (eq. 4-6):

$$L^- = \sum_{K=1}^3 L_K^- ((\rho_K)^{obs}) \quad (\text{eq. 4})$$

with:

$$L_K^- ((\rho_K)^{obs}) = \frac{1}{2} \sum_{i,j,t,\Omega} [\ln((\rho_K)_{i,j,t,\Omega}^{obs}) - \ln((\rho_K)_{i,j,t,\Omega}^{pred})]^2 \quad (\text{eq. 5})$$

for $K = 1$ and 2 , and since the sum of ratios is 1:

$$L_K^- ((\rho_K)^{obs}) = \frac{1}{2} \sum_{i,j,t,\Omega} [\ln(1 - (\rho_K)_{i,j,t,\Omega}^{obs}) - \ln(1 - (\rho_K)_{i,j,t,\Omega}^{pred})]^2 \quad (\text{eq. 6})$$

for $K = 3$.

Revised adjoint code was manually written and then compared to results obtained with an automatic differentiation library (AUTODIFF, Otter Research Ltd., 1994) and validated by a derivative check, i.e., we verify (eq. 7) that the discrepancy between each gradient component (obtained by analytic differentiation (adjoint code) and its finite difference approximation changes parabolically with step h varying from 10^{-8} to 10^{-2} (Senina et al., 2008).

$$\forall n, \frac{L^-(E_n' + h) - L^-(E_n' - h)}{2h} - \nabla_k L^- = O(h^2) \quad (\text{eq. 7})$$

Each parameter E'_n is allowed to vary between 0 and 1 and then rescaled to fulfill the condition of their sum being equal to 1 at the end of each likelihood function evaluation.

Finally, the general approach was validated with twin experiments. In such experiments, pseudo-observations are extracted from biomass outputs predicted from a run of the model (Fig. 5) with an initial parameterization (P_{init}). They are used to verify that after changing the parameter values the model can converge towards the exact original values of parameters. Once the convergence criterion is reached, the relative error to the exact value (e_n) is calculated following equation 8:

$$e_n = \frac{|\widehat{E}'_n - E'_n|}{E'_n} \quad (\text{eq. 8})$$

For a first series of 5 twin experiment simulations we used pseudo-observations extracted along the Hawaiian transect. Then, 16 series of 5 replicate simulations were produced with pseudo-observations randomly distributed either on 1, 3, 5 or 10 time steps of the simulation and 20, 50, 100 or 200 localizations by time step. Thus, a total of 85 twin experiment simulations were conducted with a range of data between a minimum of 20 and a maximum of 2000 observations. To compare the results, we first used the mean negative-log likelihood value of each group of 5 simulations. In addition, we also computed the relative standard deviation of the negative log likelihood ($\sigma L^- / \overline{L^-}$) for each group of 5 replicate simulations to compare between these groups while accounting for their different averages ($\overline{L^-}$) and numbers of observations.

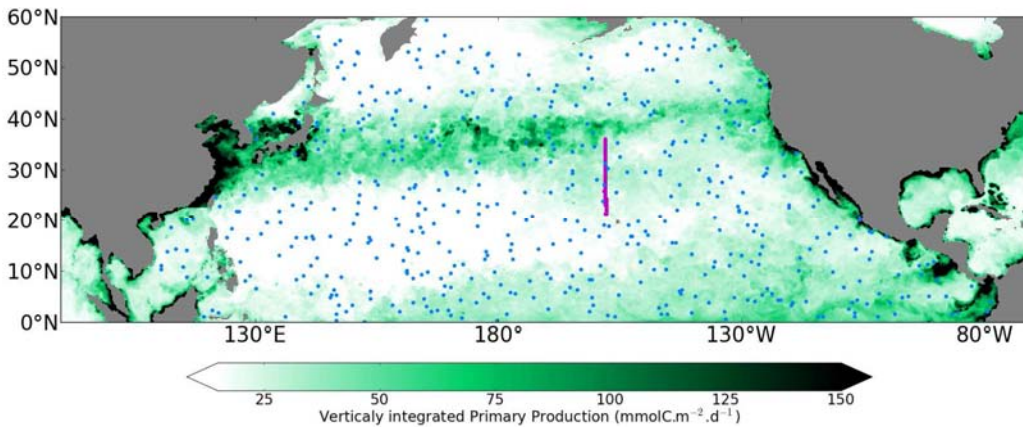


Figure 5: Distribution of pseudo-observations for twin experiments either along the Hawaiian transect (pink ticks) or distributed according a random sampling on position and period of day (blue dots), superimposed on primary production deduced from ocean color data.

Results

6. Twin experiments

All twin experiments are run from an initial parameterization with all E'_n coefficients set to $1/6^{\text{th}}$, and with the same number of night and day pseudo-observation to avoid any potential bias. Overall, the

level of error on parameter estimates decreased with the number of pseudo-observations included in the experiment, from a maximum relative error of $\sim 10\%$ in the worst case with 20 to 50 pseudo-observations to less than 1% in the best case with maximum spatial and temporal coverage. A minimum of 200 pseudo-observations appeared necessary to remain below the threshold of 5% error (Fig. 6).

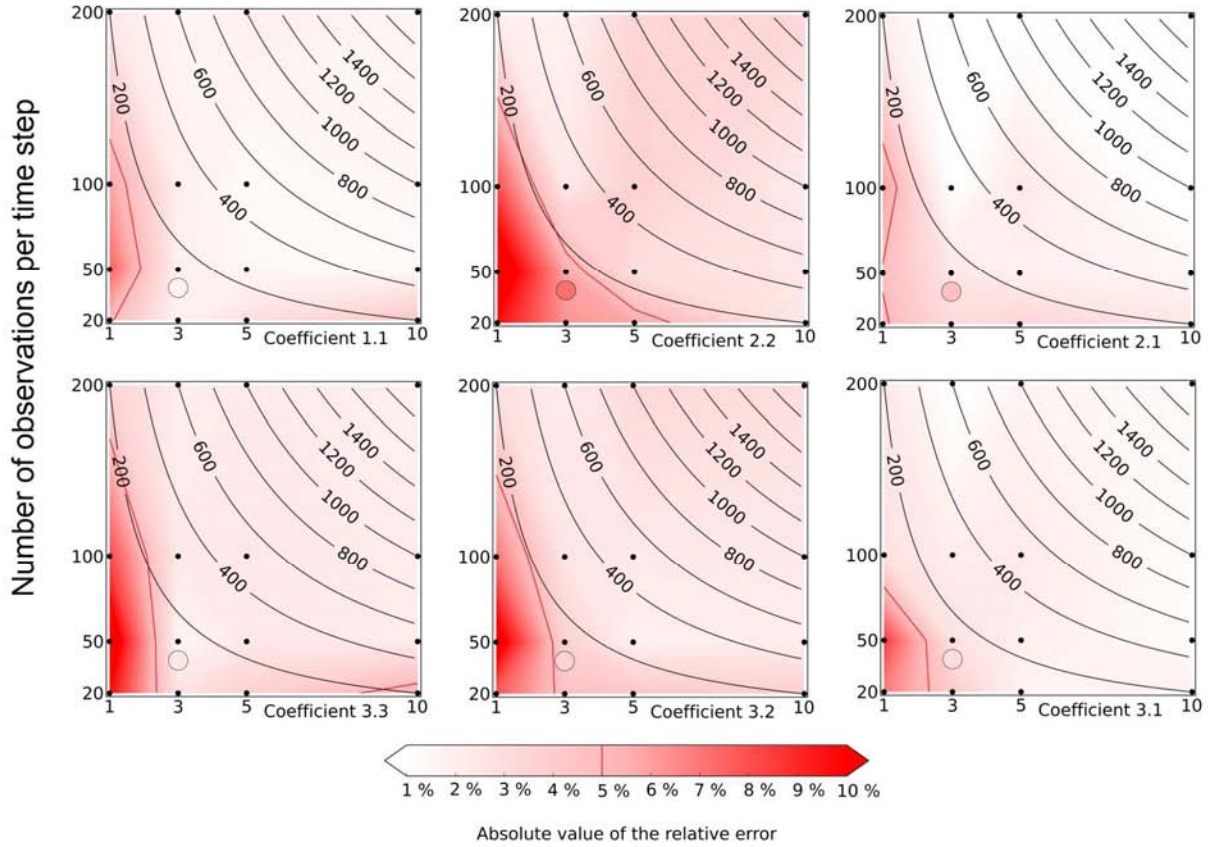


Figure 6: Mapping of the average absolute value of the relative error (e_n) for each coefficient E'_n in the retrieval of parameters in twin experiments (identified with black dots), over temporal (horizontal axis) and spatial resolution (vertical axis). Black curves show isolines with same numbers of pseudo-observations. Red lines delineate the five-percent relative error area. Circles show the location of relative errors of twin experiments that mimic the actual Hawaiian transect.

The response of the model showed a dissymmetry considering the number of pseudo-observations included either spatially or temporally. For the same number of pseudo-observations it is better to have these data along the same transect but over several time steps than well dispersed over a single time step (Fig. 6). Each group had its own response in the variance of estimated error, the most sensitive being the non-migrant upper mesopelagic group (2.2). The three groups that inhabit at least during night-time the epipelagic layer, i.e., the epipelagic (1.1), migrant upper mesopelagic (2.1) and highly-migrant lower mesopelagic (3.1) groups were those that have the lowest level of error (Fig. 6), followed by the non-migrant lower mesopelagic group (3.3) and finally the migrant lower mesopelagic (3.2) and the non-migrant upper mesopelagic (2.2) groups. These different responses could be related to more dynamic and contrasted signals in the epipelagic layer with higher temperature and stronger currents. This is certainly not the case for the non-migrant lower mesopelagic group, but this one has

the advantage to stay alone in its layer at night with clear information on its biomass ratio. In the upper mesopelagic layer the signal is less clear since it always results from a combination of two different groups and the turnover and dynamics are relatively slow. The result for the twin experiments imitating the actual Hawaiian transect, i.e., with same number and localization of pseudo-observations, is shown in Fig. 6 and confirms the general pattern with the largest error for the group 2.2 (7.14%) while it is below 5% for the others. The error on the coefficient of group 2.1 (4.64%) is slightly above what is expected.

The total negative log-likelihood increased with the number of pseudo-observations included in the twin experiments (Fig. 7). This is not surprising since even with small errors their sum increases with the number of observations. However, it increased homogeneously and symmetrically on both time and space axes. The value for the samples that mimic the actual Hawaiian transect is below the expected value, possibly due to a favorable position of the transect crossing contrasted systems, i.e., the tropical gyre and the Convergence Zone of Chlorophyll (Polovina et al. 2001).

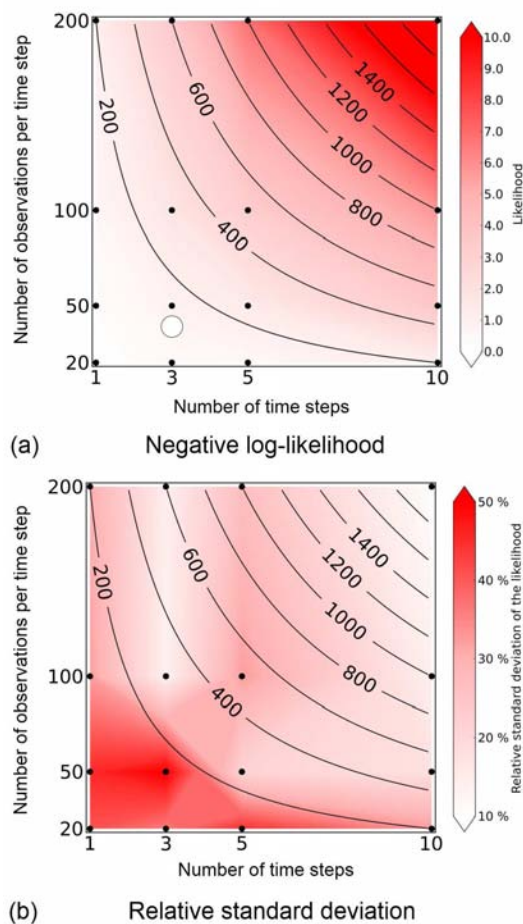


Figure 7: Mapping of the mean negative log-likelihood (a) and relative standard deviation of the negative log-likelihood (b), over temporal (horizontal axis) and spatial resolution (vertical axis). Black curves show isolines with same numbers of pseudo-observations and circle on a) shows the location of the mean negative log-likelihood that mimics the actual Hawaiian transect.

The standard deviation of the negative log-likelihood once corrected to the total number of observations allowed for the analyses of the intra-samples variability independently from their size. This relative standard deviation showed the largest deviation ($> 35\%$ of the log-likelihood) for small size samples (Fig. 7). Again the amount of 200 observations appeared as a rough minimum threshold, a result also confirmed by the Bayesian information criterion (Akaike 1974, Schwarz 1978) that account for the number of observations and parameters (Fig. 8), the latter being fixed in our case.

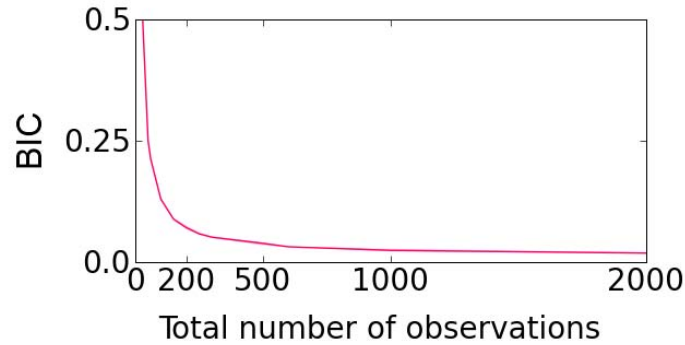


Figure 8: Bayesian information criterion (BIC) computed for all twin experiments.

7. Estimated parameters with Hawaiian transect

At the resolution of the model, i.e., $\frac{1}{4}^\circ \times \text{week}$, the transect used to run the real optimization experiment provided 116 observations over 3 consecutive time steps. The model successfully converged with a new parameterization with new coefficient values distributed over a larger range (0 to 0.435) than for the initial parameterization (Table 1). Coefficients of lower and highly-migrant lower mesopelagic groups showed the largest increase with estimates between boundary values. Conversely, estimates for the groups of the upper mesopelagic layer strongly decreased and even reached 0 for the non-migrant group (Table 1). The coefficient value of the non-migrant lower mesopelagic was also estimated at the boundary. Therefore, this first optimization is not entirely satisfying, possibly because of the small number of observations and the uncertainty on forcing variables (see also discussion).

Table 1: Matrix of the energy coefficients transfer used for the 3-layer 6-component MTL model according to the functional group and the number of vertical layers, and for different simulation experiments. 1: parameterisation achieved from the literature (Lehodey et al 2010a); Opt: optimisation after data filtering and 5% of the biomass added in the epipelagic.

Nb of layer	Simulation experiment	Epi	Upper Meso	Migrant Upper meso	Lower meso	Migrant Lower Meso	Highly Migrant Lower Meso
0 (land)	All	0	0	0	0	0	0
1	All	1	0	0	0	0	0
2	1	0.340	0.270	0.390	0	0	0
	Opt	0.463	0.310	0.227	0	0	0
3	1	0.170	0.100	0.220	0.180	0.130	0.200
	Opt	0.236	0.083	0.000	0.435	0.020	0.226

Nevertheless, even though the new optimized parameterization should be considered very preliminary, it improved the average overall fit to observed ratios in the 3 layers (Fig. 9). The low values of signal ratios in the upper mesopelagic layer and its weak variability may explain the difficulty to retrieve correct estimates of energy transfer coefficients for the groups inhabiting this layer. In addition, spatial and temporal resolution of the model still cannot predict the level of variability observed. The model also does not resolve the transition phase during twilight hours. Finally, other various sources of uncertainty that are inherent to the model and its forcing, as well as in the acoustic data, are detailed in the discussion.

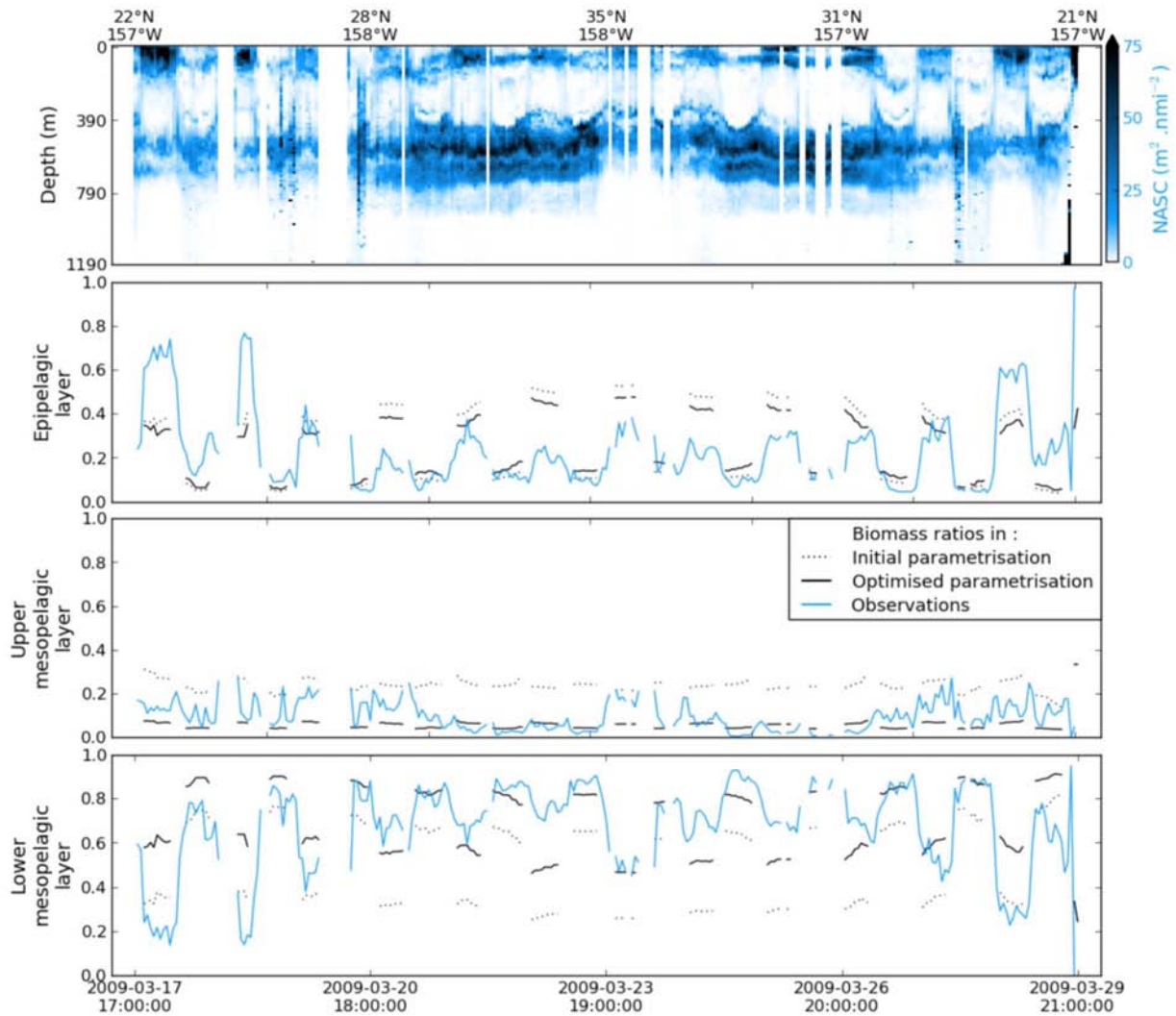


Figure 9: Comparison between observations and predictions. First panel shows the whole acoustic transect (averaged over a one-hour period) in NASC (Nautical Area Scattering Coefficient). The three other panels shows biomass ratios in the corresponding layer (averaged over a one-hour period): blue lines for observed, black dotted lines for parameterization published in Lehodey et al. (2010a) and black solid lines for the new optimization.

However, one striking disagreement between observed and predicted ratios occurred at the beginning and end of the Hawaiian transect, i.e., when leaving and returning to the Hawaiian Islands. The model could not predict the high values observed during the night in the epipelagic layer and, conversely, the low values in the lower mesopelagic layer. A more detailed investigation detected a potential problem associated with the mesoscale activity. Although the currents predicted with the GLORYS reanalysis compared fairly well with those deduced from altimetry data (Fig 10), the detailed mesoscale features might differ substantially locally. For example, the very high ratio value in the epipelagic layer at night occurring at 25°N along the transect (Fig 9) seemed to coincide with a structure of two small eddies of opposite rotation that are visible on the altimetry map but not in the predicted currents of GLORYS (Fig. 10). This type of structure associating one cyclonic and one anti-cyclonic mesoscale eddy is highly favorable to the concentration of organisms in the area of convergence of currents as predicted for instance in the south-east corner of the micronekton biomass distribution map on figure 10d. The lack of such a structure at 25°N on the transect in the field of predicted currents used to simulate the micronekton could explain the too low micronekton biomass predicted by the model in comparison to acoustic data.

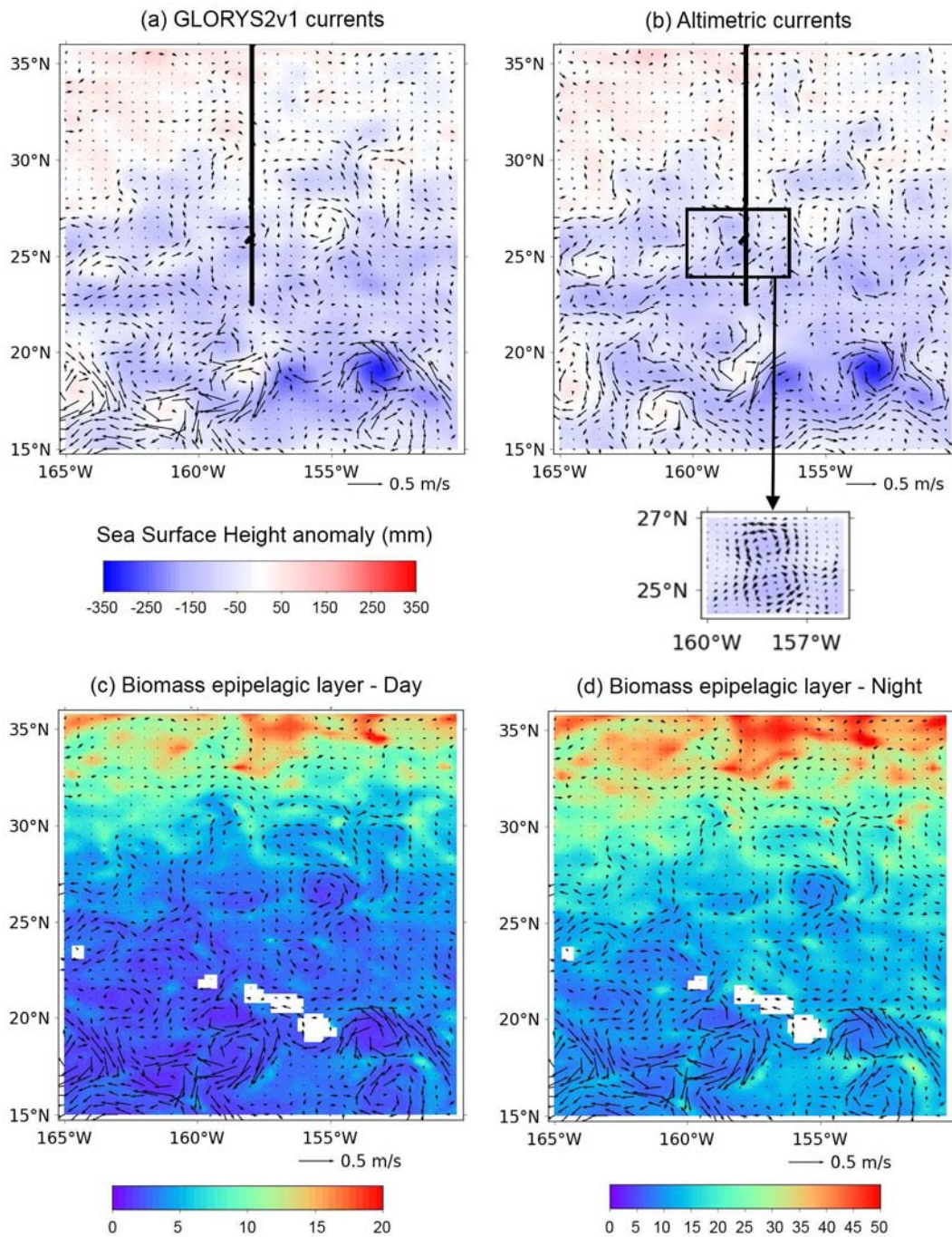


Figure 10: Mesoscale prediction and observation. (a) Current velocity (arrows) from GLORYS2v1 reanalysis (week of 16-22 March, 2009) superimposed on observed sea surface height (SSH) anomaly (AVISO CNES/CLS <http://www.aviso.oceanobs.com/>); (b) Current velocity (arrows) deduced from altimetry for the same period and also superimposed on SSH. The acoustic transect (black line) is superimposed and a zoom is shown for the area identified with a rectangle. (c) Predicted biomass distribution in the epipelagic layer during daytime and (d) during nighttime with superimposed GLORYS2v1 currents. Note the different ranges of values between color bars.

Discussion

Acoustic sampling is the only available approach to collecting a sufficient amount of data at basin scales. At first glance, it shows micronekton distribution and density that is globally still missing today. However, even with a vast sampling effort, it could not offer the synoptic view that is required for understanding and eventually managing these huge oceanic ecosystems. Therefore, the data need to be complemented with ecological models with appropriate levels of detail and parameters tailored to match this type of data. This study provides a methodology for a simple and robust use of acoustic data in an original parsimonious model of micronekton functional groups.

Acoustic data initially allowed us to define the vertical boundaries of the 3 biological layers in the model. Such a definition is critical as physical variables that drive the dynamics of MTL groups are averaged within these layers. Ongoing work in other oceanic basins (e.g., the Southern Indian Ocean) suggests that this definition could be generalized at the ocean basin scale, although this question of vertical boundaries remains fully open and will require many other acoustic transects and research cruises from various oceanic regions and seasons to be confirmed.

Clearly, the initial optimal parameterization achieved here with one single transect and single frequency is preliminary, and new experiments will have to be conducted with more data and acoustic interpretation. The approach based on relative signal ratios should help in combining different data sources, but this assumes no horizontal and vertical bias in the acoustic measurement and their biological interpretation. Reducing vertical and horizontal bias from the acoustic measurements can be achieved with modern calibrated echo sounders from research and fishing vessels with the data available with appropriate metadata (Kloser et al. 2009, www.imos.org.au, ICES 2013). Thus, it is necessary to implement automatic data screening to remove obvious wrong signals and filtering so as to avoid spurious integration of noise (e.g., De Robertis and Higginbottom 2007). It is also essential that the treatment of the signal along the vertical dimension be comparable with appropriate beam spreading compensation and absorption correction for the frequency used (Francois and Garrison 1982). Adjustments need to be made for potential changes in transducer sensitivity and absorption in the horizontal direction that are mainly a result of temperature (Demer and Renfree 2008). This data processing method then enables a comparison of acoustic backscatter ratios between depths and regions. To compare data sets from different instruments and regions, the data metadata must describe the instrument, the calibration, and signal processing methods used (ICES 2013).

This work has assumed that the biological interpretation of the acoustics contains no vertical or horizontal bias and that the acoustic signal is proportional to the micronekton biomass at all depths (Benoit-Bird and Au 2002). This will not be the case at lower frequencies, such as 38 kHz used here, as a result of resonance scattering effects in the mesopelagic layer from fish and siphonophores with gas inclusions in particular. For example, at 600 m depth the backscatter at 38 kHz can be an order of magnitude higher than the 120 kHz frequency as used by Benoit-Bird and Au (2002) requiring a scaling adjustment (Kloser et al. 2002). To accurately compare data from different layers and between different regions, the proper ratios of different types of micronektonic organisms and their sizes must be estimated, and adjustments must be made for differences in acoustic backscatter based on composition and size (Handegard, et al. 2013). This is true even if all micronektonic groups, i.e., fish with and without gas-bladder, crustaceans, cephalopods, and gelatinous organisms with and without gas inclusions (e.g. some siphonophores), are considered as a whole as in this study. Advances in multi-frequency acoustics and detailed studies on the conversion of acoustic to biological units are required to narrow down the range of errors and biases based on resonance scattering. The calibration of diffusion parameter needs also to be investigated through sensitivity analysis. Decreasing its value would certainly reinforce the contrast in the predicted biomass ratio but likely could make the model convergence more difficult to achieve.

Our estimate of epipelagic biomass may be biased low as a result of the near-surface region unsampled by the acoustics (~ 15 m depth) or affected by vessel avoidance (e.g., O'Driscoll, et al. 2009, De Robertis, A., and Handegard, N.O. 2013). This bias may have a spatial and temporal structure and be region-specific depending on the species present. In this initial experiment we arbitrarily fixed the missing near-surface biomass to 5% of the total signal, which is only a first-guess estimate. Based on 38 kHz acoustic data collected along a circumnavigation, Irigoien et al. (2014) give an estimate of 7% for the biomass in the upper 200 m after excluding 5 areas with exceptional high values. To explore the magnitude of this bias will require methodological and technological solutions. Using the existing echo sounder data it is possible to observe the migration behavior of the species to determine the potential extent of the problem and the need for higher compensation or dedicated near-surface sampling technology (O'Driscoll, et al. 2009). Examples of available near-surface acoustic technology are upward-looking echo sounders (moored or mobile) and sideways-looking sonars (Handegard et al., 2013). Estimating biomass from these devices is complicated by the need to know the target strength of the species at different orientations. At the least these devices can detect the relative change of acoustic signal above and below the near-surface region to explore the potential magnitude of the bias. Sampling the near surface with acoustics also has some physical constraints due to the instruments pulse length, waves and bubbles. Uncertainty in biomass estimates from these issues will need to be addressed if precise epipelagic biomass estimates are to be obtained. Despite all these raised issues, observing the behavior of the vertical migration of mesopelagic organisms could be the best method to highlight the potential magnitude of the problem to direct more research.

With the quality and coverage of acoustic data, forcing fields are another area for increasing the accuracy of the model in simulating the dynamics of micronekton functional groups. The twin experiments indicated that 200 observations could be sufficient to retrieve the correct parameter values. However, this is for the ideal and theoretical case of a perfect environmental forcing, i.e., here the same used both for producing pseudo-observations and running optimization. In practice, there are many sources of uncertainties on the variables used to reproduce the oceanic environment.

The VGPM model of primary production that is used here is one among many satellite "chlorophyll-based" models with empirically determined functions that are generalized to basin scale. For instance, an alternative definition of the temperature-dependent photosynthetic efficiencies as suggested by Eppley (1972) leads to substantial differences in the estimates (see <http://www.science.oregonstate.edu/ocean.productivity/>). The accuracy of 21 ocean color models was recently assessed by comparing their estimates to *in situ* measurements (Saba et al. 2011). While on average, simple and more complex models had similar performances, their average accuracy was significantly higher at seabed depths greater than 250 m, i.e., for the Case-1 (pelagic) waters used in our study. Therefore, primary production estimates are likely degraded close to the coast and these errors can cascade downstream and propagate offshore.

Similarly ocean circulation models still have biases or drifts from observations despite the assimilation of satellite and available *in situ* data (Lellouche et al 2012; Ferry et al 2012). These sources of errors likely increase with depth in relation to the number of observations available for assimilation, and also near the coast due to the necessity of degrading the actual topography at the resolution of the model grid ($1/4^\circ$). The discrepancy observed in this study between mesoscale features predicted by the reanalysis or deduced from altimetry is a good illustration of these potential sources of errors with a direct consequence on the micronekton estimate. However, it is worth noting that the optimization procedure improved the average estimate independently of these local errors. This suggests that the method is robust and can account for these sources of errors.

The next step will consist in optimization experiments based on longer time series and with a larger amount of observations needed to compensate the various sources of uncertainties. Given the effort developed with the IMOS initiative (Kloser et al. 2009; <http://www.imos.org.au/>) to collect 38 kHz and other acoustic frequency data routinely, it is envisaged to develop a configuration for the southern hemisphere and use all these available and standardized data. New fine-scale acoustic, optical and trawling regional-based experiments are needed to interpret this broader spatial and temporal scale acoustics data to initialize and assimilate into the model (Handegard et al. 2013). In particular, experiments to quantify the conversion of acoustic backscatter into biological units accounting for resonance scattering are needed. The optimal parameterization will be then used for a global hindcast simulation allowing evaluation of the results in the northern hemisphere with historical data, e.g., the MARECO platform. It is also worth noting that our twin experiments suggest that a long time series of acoustic data in a single point could provide more useful information for parameter optimization than the same amount of data spatially dispersed over a few time steps. It is essential to confirm or not this result given its potential consequences when designing ocean-monitoring networks.

Parallel to the progress of acoustic technology and associated validation experiments for quantifying and discriminating between the major groups of micronekton organisms, the model could be further developed easily to account for a more detailed description of the pelagic mid-trophic levels.

Acknowledgments

The authors wish to thank the Groupe Mission Mercator Coriolis and the GLORYS members (MERCATOR-OCEAN, INSU-CNRS and the team “DRAKKAR”) for providing the GLORYS-2v1 reanalysis. We also thank the Ocean Productivity team for providing us the SeaWiFS-derived primary production. This study was partially supported by a grant from the US JIMAR Pelagic Fisheries Research Program and by the FP7 EU Euro-BASIN research project. We are also grateful to two anonymous reviewers who provided useful comments to improve a first version of the manuscript.

References

- Abecassis, M., Senina, I., Lehodey, P., Gaspar, P., Parker, D., Balazs, G., and Polovina, J. 2013. A Model of Loggerhead Sea Turtle (*Caretta caretta*) habitat and movement in the oceanic North Pacific. *PLoS ONE*, 8: e73274.
- Akaike, H. 1974. A new look at the statistical model identification. *IEEE Transactions on Automatic Control*, 19: 716–723.
- Barnier, B., Madec, G., Penduff, T., Molines, J. -M., Treguier, A. -M., le Sommer, J., Beckmann, A., et al. 2006. Impact of partial steps and momentum advection schemes in a global ocean circulation model at eddy permitting resolution. *Ocean Dynamics*. doi:10. 1007/s10236-006-0082-1
- Behrenfeld, M. J., and Falkowski, P. G. 1997. A consumer’s guide to phytoplankton primary productivity models. *Limnology and Oceanography*, 42: 1479–1491.
- Benoit-Bird, K. J., and Au, W. W. L. 2002. Energy: converting from acoustic to biological resource units. *Journal of the Acoustical Society of America*, 111: 2070–2075.
- Brasseur, P., Gruber, N., Barciela, R., Brander, K., Doron, M., El Moussaoui, A., Hobday, A., et al. 2009. Integrating biogeochemistry and ecology into ocean data assimilation systems. *Oceanography*, 22: 206–215.
- Briand, K., Molony, B., and Lehodey, P. 2011. A study on the variability of albacore (*Thunnus alalunga*) longline catch rates in the south-west Pacific Ocean. *Fisheries Oceanography*, 20: 517–529.
- Demer, D. A., and Renfree, J. S. 2008. Variations in echosounder–transducer performance with water temperature. *ICES Journal of Marine Science*, 65: 1021–1035.

- De Robertis, A., and Higginbottom, I. 2007. A post-processing technique to estimate the signal-to-noise ratio and remove echosounder background noise. *ICES Journal of Marine Science*, 64: 1282–1291.
- De Robertis, A., and Handegard, N. O. 2013. Fish avoidance of research vessels and the efficacy of noise-reduced vessels: a review. *ICES Journal of Marine Science*, 70: 34–45.
- deYoung, B., Heath, M., Werner, F., Chai, F., Megrey, B., and Monfray, P. 2004. Challenges of modeling ocean basin ecosystems. *Science*, 304: 1463–1466.
- Downey, E. C. 1990. XEphem Version 3.7.6 Reference Manual. <http://www.clearskyinstitute.com/xephem/> (last accessed 12 December 2014).
- Dueri, S., Faugeras, B., and Maury, O. 2012. Modelling the skipjack tuna dynamics in the Indian Ocean with APECOSM-E: Part 1. Model formulation. *Ecological Modelling*, 245: 41–54.
- Eppley, R.W. 1972. Temperature and phytoplankton growth in the sea. *Fishery Bulletin*, 70: 1063–1085.
- Ferry, N., Parent, L., Garric, G., Drevillon, M., Desportes, C., Bricaud, C., and Hernandez, F. 2012. Scientific validation report (ScVR) for reprocessed analysis and reanalysis. MyOcean project report, MYOWP04-ScCV-rea-MERCATOR-V1.0. 66 pp. <http://www.mercatorocean.fr/fre/Media/Files/GLORYS/MYO-WP4-ScVR-rea-MERCATORV1.0.pdf> (last accessed 19 December 2014).
- Foote, K. G., Knudsen, H. P., Vestnes, G., MacLennan, D. N., and Simmonds, E. J. 1987. Calibration of acoustic instruments for fish density estimation: a practical guide. *ICES Cooperative Research Report*, 144, 69 pp.
- Francois, R. E., and Garrison, G. R. 1982. Sound absorption based on ocean measurements. Part II: Boric acid contribution and equation for total absorption. *The Journal of the Acoustical Society of America*, 72, 1879, <http://dx.doi.org/10.1121/1.388673> (last accessed 19 December 2014).
- Fulton, E. A. 2010. Approaches to end-to-end ecosystem models. *Journal of Marine Systems*, 81: 171–183.
- Grandperrin, R. (1975), Structures trophiques aboutissant aux thons de longue ligne dans le Pacifique Sud-Ouest, Thèse de doctorat de l'Université d'Aix-Marseille II, 295p.
- Handegard, N. O., du Buisson, L., Brehmer, P., Chalmers, S. J., De Robertis, A., Huse, G., Kloser, R. et al. 2013. Towards an acoustic-based coupled observation and modelling system for monitoring and predicting ecosystem dynamics of the open ocean (2012). *Fish and Fisheries*, 14(4): 605–615.
- Holt J., Allen J. I., Anderson T. R., Brewin, R., Butenschon M., Harle J., Huse G., Lehodey, P., Lindemann C, Memery L., Salihoglu B., Senina I., Yool A. (2014). Challenges in integrative approaches to modelling the marine ecosystems of the North Atlantic: Physics to Fish and Coasts to Ocean. *Progress in oceanography*, <http://dx.doi.org/10.1016/j.pocean.2014.04.024>
- ICES 2013. A metadata convention for processed acoustic data from active acoustic systems, SISP 3 TG-AcMeta, ICES GFAST Topic Group, TG-AcMeta. 35pp.
- Irigoien X., Klevjer T.A., Rostad A., Martinez U., Boyra G., Acuña J.L., Bode A., Echevarria F., Gonzales-Gordillo J.I., Hernandez-Leon S., Agusti S., Aksnes D.L., Duarte C.M., Kaartvedt S. (2014). Large mesopelagic fishes biomass and tropic efficiency in the open ocean. *Nature Communications* 5 (3271), DOI:10.1038/ncomms4271
- Jennings, S., Mélin, F, Blanchard, J.L., Forster, R.M., Dulvy, N.K., Wilson R.W. (2008). Global-scale predictions of community and ecosystem properties from simple ecological theory. *Proc. R. Soc. B* 275, 1375–1383 doi:10.1098/rspb.2008.0192.
- Kitchell J.F., Boggs C.H., He X., Walters C.J. (1999). Keystone predators in the Central Pacific. *Proceedings of the Symposium on Ecosystem Considerations in Fisheries Management*, Sep 30–Oct 3, Anchorage, Alaska, USA. Alaska Sea Grant College Program. AK-SG-99-01: pp 665–68.

- Kloser, R. J., Ryan, T., Sakov, P., Williams, A., and Koslow, J. A. 2002. Species identification in deep water using multiple acoustic frequencies. *Canadian Journal of Fisheries and Aquatic Sciences*, 59: 1065–1107.
- Kloser, R. J., Ryan, T. E., Young, J. W., and Lewis, M. E. 2009. Ocean-basin scale acoustic observations of micronekton fishes: potential and challenges. – *ICES Journal of Marine Science*, 66 (6): 998-1006.
- Lambert C., Mannocci L., Lehodey P., Ridoux V. 2014. Predicting cetacean habitats from their energetic needs and the distribution of their prey in two contrasted tropical regions. *PLoS ONE* 9(8): e105958. doi:10.1371/journal.pone.0105958.
- Lehodey P., Murtugudde R., Senina I. 2010a. Bridging the gap from ocean models to population dynamics of large marine predators: a model of mid-trophic functional groups. *Progress in Oceanography*, 84: 69–84.
- Lehodey P., Senina I., Calmettes B, Hampton J, Nicol S. 2013. Modelling the impact of climate change on Pacific skipjack tuna population and fisheries. *Climatic Change*, 119 (1): 95-109.
- Lehodey P., Senina I. and Murtugudde R. 2008. A Spatial Ecosystem And Populations Dynamics Model (SEAPODYM) - Modelling of tuna and tuna-like populations. *Progress in Oceanography*, 78: 304-318.
- Lehodey P., Senina I., Sibert J., Bopp L, Calmettes B., Hampton J., Murtugudde R. 2010b. Preliminary forecasts of population trends for Pacific bigeye tuna under the A2 IPCC scenario. *Progress in Oceanography*. 86: 302–315.
- Lellouche, J.-M., Le Galloudec, O., Drévilion, M., Régnier, C., Greiner, E., Garric, G., Ferry, N., Desportes, C., Testut, C.-E., Bricaud, C., Bourdallé-Badie, R., Tranchant, B., Benkiran, M., Drillet, Y., Daudin, A., and De Nicola, C. 2012. Evaluation of real time and future global monitoring and forecasting systems at Mercator Océan, *Ocean Sci. Discuss.*, 9(2): 1123-1185.
- Mac Lennan, D. N., Fernandes P. G., Dalen J. 2002. A consistent approach to definitions and symbols in fisheries acoustics, *ICES Journal of Marine Science*, 59, 365-369.
- Maury, O. 2010. An overview of APECOSM, a spatialized mass balanced “apex predators ECOSystem model” to study physiologically structured tuna population dynamics in their ecosystem. In: John, M., Monfray, P.St. (Eds.), *Parameterisation of Trophic Interactions in Ecosystem Modelling. Progress in Oceanography* 84, 113–117.
- O’Driscoll, R. L., Gauthier, S., and Devine, J. A. 2009. Acoustic estimates of mesopelagic fish: as clear as day and night? *ICES Journal of Marine Science*, 66: 1310–1317.
- Pham, D. T., Verron, J., Roubaud, M.C. 1998. A singular evolutive extended Kalman filter for data assimilation in oceanography, *Journal of Marine Systems*, 16, 323-340.
- Plagányi, É. E. 2007. Models for an Ecosystem Approach to Fisheries. FAO Fisheries Technical Paper, No. 477. FAO, Rome, 108 p.
- Polovina JJ, Howell E, Kobayashi DR, Seki M.P. 2001. The transition zone chlorophyll front, a dynamic global feature defining migration and forage habitat for marine resources. *Progress in Oceanography*, 49: 469–483.
- Saba V. S., Friedrichs M. A. M., Antoine D., Armstrong R. A., Asanuma I., Behrenfeld M. J., A Ciotti. M., Dowell M., N. Hoepffner, W. Hyde K. J. , Ishizaka J., Kameda T., Marra J., Melin F., Morel A., O’Reilly J., Scardi M., Smith Jr. W. O., Smyth T. J., Tang S., Uitz J., Waters K., Westberry T. K. 2011. An evaluation of ocean color model estimates of marine primary productivity in coastal and pelagic regions across the globe. *Biogeosciences*, 8, 489–503.
- Schwarz, G. E. 1978. "Estimating the dimension of a model". *Annals of Statistics* 6 (2): 461–464.
- Senina I., Sibert J. and Lehodey P. 2008. Parameter estimation for basin-scale ecosystem-linked population models of large pelagic predators: application to skipjack tuna. *Progress in Oceanography*, 78: 319-335.

- Sibert J, Senina I, Lehodey P, Hampton J. 2012. Shifting from marine reserves to maritime zoning for conservation of Pacific bigeye tuna (*Thunnus obesus*). *Proceedings of the National Academy of Sciences* 109(44): 18221-18225.
- Tranchant, B., Testut, C.-E., Renault, L., Ferry, N., Birol, F., Brasseur P. 2008. Expected impact of the future SMOS and Aquarius Ocean surface salinity missions in the Mercator Ocean operational systems: New perspectives to monitor the ocean circulation. *Remote Sensing of Environment*, 112, 1476-1487.